on the acoustic radiation on the basis of numerical calculations in the investigated situation.

The authors are grateful to V. A. Gushchin for supplying the program used to calculate the hydrodynamic characteristics of a collapsing blob.

[1])The importance of collapse-type processes for the excitation of acoustic oscillations by vortex disturbances in a stratified medium was first noted in Ref. 6 (see also Ref. 7).

[1] A. V. Furduev, "Ocean noise," in: Ocean Acoustics [in Russian], L. M. Brekhovskikh (ed.), Nauka, Moscow (1974), pp. 615-692.

[2] G. I. Barenblat, Izv. Akad. Nauk SSSR Fiz. Atm. Okeana 14, 195 (1978).

[3] V. S. Maderich, V. I. Nimeshov, and A. T. Stetsenko, Dynamics of Internal Mixing in a Stratified Medium [in Russian], Naukova Dumka, Kiev (1988).

[4] V. A. Gushchin, Zh. Vychisl. Mat. Mat. Fiz. 21, 1003 (1981).

[5] S. O. Belotserkovskii and V. A. Gushchin, Modeling of Certain Viscous Fluid Flows, Preprint of the Computing Center of the Academy of Sciences of the USSR [in Russian], VTs AN SSSR (1982).

[6] L. M. Lyamshev and A. T. Skvortsov, Akust. Zh. 30, 843 (1984) [Sov. Phys. Acoust. 30, 503 (1984)].

[7] L. M. Lyamshev and A. T. Skvortsov, "Sound radiation by localized vortices in a slightly compressible medium (review)," Akust. Zh. 34, 769 (1988) [Sov. Phys. Acoust. 34, 447 (1988)].

[8] M. J. Lighthill, Proc. R. Soc. London Ser. A 222, 1 (1954).

[9] L. M. Brekhovskikh and V. S. Goncharov, Mechanics of Continua and Wave Dynamics, Springer-Verlag, Berlin–New York (1985).

[10] M. E. Goldstein, Aeroacoustics, McGraw-Hill, New York (1976).

[11] B. P. Demidovich and I. A. Maron, Fundamentals of Computational Mathematics [in Russian], Nauka, Moscow (1970).

[12] A. A. Samarskii, Theory of Difference Schemes [in Russian], Nauka, Moscow (1983).

[13] Yu. P. Doronin (ed.), Physics of the Ocean [in Russian], Gidrometeoizdat, Leningrad (1978).

Translated by J. S. Wood

Directivity patterns of a spark source of acoustic waves in a solid

S. V. Korolev and V. V. Krylov

Physics Department, M. V. Lomonosov State University, Moscow

(Submitted February 13, 1989)

Akust. Zh. **36**, 42–47 (January–February 1990)

The directional characteristics of a spark source of acoustic waves in a solid are studied experimentally. The angular dependence of the amplitudes of longitudinal and shear waves and of Rayleigh surface waves is investigated for two principal discharge geometries. A qualitative interpretation of the observed dependences is given.

The last few years have witnessed a heightened interest in various noncontact methods for the generation of sound in solids: electromagnetic,[1,2] laser,[3-5] and other methods. One of the more promising noncontact methods, proposed quite recently, is the so-called spark method, or the generation of sound in solids by electrical breakdown of the surface air layer.[6-9] Foremost among the advantages of this generation technique over other noncontact methods, e.g., over the laser method, is the simplicity of implementation, compactness, low cost, and higher efficiency. According to Ref. 7, the principal mechanism of the spark generation of acoustic waves in a solid is the exposure of its surface to the strong divergent air shock produced by expansion of the discharge plasma. Since the characteristic duration of the air-shock pulse near the discharge zone can be fairly small (of the order of a few tens of nanoseconds); the excited shock pulses can also be very short.[9] This means that the spark method can be used for spectral measurements of the parameters of solids, in particular for ultrasonic spectroscopy and nondestructive testing.

Among the most important properties of any acoustic wave source are its directivity patterns. In application to the spark generation of sound, the first experimental study of the angular dependence of the radiated field was reported in Ref. 6. However, the measurements in Ref. 6 were carried out only for longitudinal waves and only with electrical discharge directly on the sample. In the present article we give the results of detailed experimental investigations of the directional characteristics of a spark source of acoustic waves in a solid. We discuss the angular dependence of the amplitudes of both longitudinal and shear waves, and also of Rayleigh surface waves for various discharge geometries and parameters. The knowledge of these dependences is essential to the practical utilization of the method in various applications. It also lends deeper insight into the nature of the spark sound source in solids.

The experiments were carried out with an aluminum sample in the shape of a half-disk of diameter 190 mm and thickness 30 mm. Electrical discharge took place both on the metal sample itself[6,7] and on an auxiliary grounded electrode.[7-9] It is important to note that the use of an auxiliary electrode permits full implementation of the noncontact method of sound generation without detracting from the purity of the surface; the sample can be either a metal or a dielectric in this case.

The experimental arrangement is shown schematically in Fig. 1. The high dc voltage source 1 generates approximately 2.7 kV. The storage

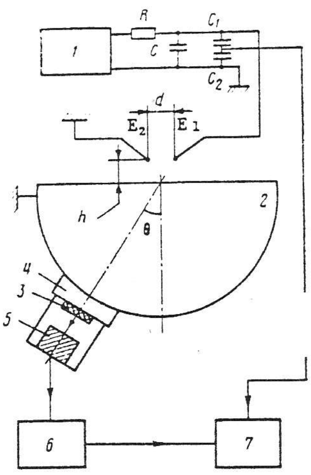

FIG. 1. Experimental arrangement.

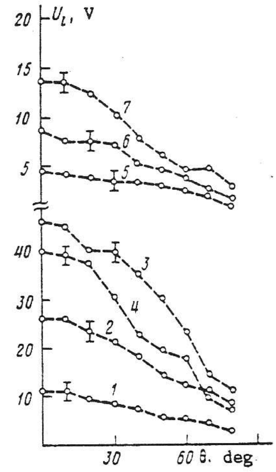

FIG. 2. Directivity patterns of longitudinal acoustic waves generated by discharge on the sample (curves 1-4) and by discharge on the auxiliary electrode (d = 0.8 mm, curves 5-7) for a capacitance C = 5200 pF. 1) h = 0.2 mm; 2) 0.3 mm; 3) 0.8 mm; 4) 0.8 mm; 5) 2 mm; 6) 1 mm; 7) 0.5 mm.

capacitor C is charged through the current-limiting resistor R ≈ 10 M Ω. The value of the capacitance C was varied in the interval from 100 pF to 35,000 pF during the measurements. The resistance R, the capacitance C, and the breakdown air gap formed a relaxation oscillator, whose frequency was varied from a few hertz to several kilohertz during the experiments. The oscilloscope sweep was triggered synchronously with electrical breakdown from the capacitative divider C_1, C_2.

The main bronze discharge electrode E_1 had a roundoff radius ~0.3 mm and was situated at a distance h from the surface of the sample 2. The value of h was varied by means of a micrometer drive, which had an error of approximately 0.03 mm. The auxiliary grounded electrode E_2 (when used) was always situated at the same distance h from the surface of the sample as the main electrode E_1; the spacing d of the electrodes was fixed at a value of approximately 0.8 mm.

The excited longitudinal acoustic wave pulses were received by the circular piezoceramic wafers 3 of diameter 15 mm with a center frequency of 2 MHz and by a lithium niobate wafer of dimensions 6 × 8 mm^2 with a center frequency of 5 MHz. Piezoceramic wafers of dimensions 6 × 10 mm^2 with a center frequency of 5 MHz were used to record the shear waves. The received longitudinal and shear waves were identified by the pulse delay times. The plastic coupling block 4, which had the same radius of curvature as the aluminum sample, was used to ensure smooth displacement of the transducers along the perimeter of the sample. Epoxy resin was used to form an acoustic bond between the coupling block and the sample.

The wideband preamplifier 5 with a low noise level and a gain of 60 dB was housed in a common metal casing with the piezoceramic plate. This arrangement made it possible to lower the stray electromagnetic noise level and, accordingly, to enhance the accuracy of the measurements. The amplified signal was subsequently transmitted to the high-pass filter 6, which lowered the noise level of the spark discharge, and then to the input of the oscilloscope 7.

The directivity patterns of the Rayleigh surface waves excited by the spark discharge were investigated on a sample in the form of an aluminum disk of diameter 300 mm and thickness 18 mm. Breakdown took place both on the sample and on the auxiliary electrode. The Rayleigh waves were received by a standard wedge transducer, to which was attached a piezoceramic wafer of diameter 15 mm with a center frequency of 2 MHz.

Figure 2 shows the angular dependence of the amplitudes of the electrical signals $U_l(\theta)$ corresponding to the generated longitudinal acoustic waves of frequency 2 MHz (curves 1-3 and 5-7) for various values of the capacitance C and the electrode height h. Curve 4 was plotted from measurement using the lithium niobate wafer with a center frequency of 5 MHz. It follows from Fig. 2 that the directivity maxima are oriented in the direction of the normal to the surface both for discharge on the sample (curves 1-4) and for discharge on the auxiliary electrode (curves 5-7), and the angular dependences themselves are similar in all cases.

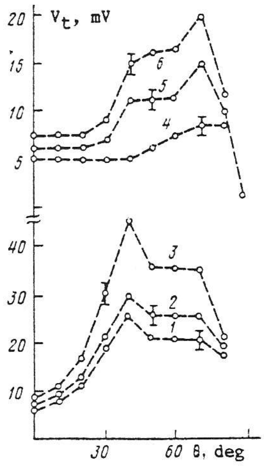

FIG. 3. Directivity patterns of shear acoustic waves generated by discharge on the sample (curves 1-3) and by discharge on the auxiliary electrode (d = 0.8 mm, curves 4-6). 1) C = 5200 pF, h = 0.4 mm; 2) C = 5200 pF, h = 0.8 mm; 3) C = 35,000 pF, h = 0.8 mm; 3) C = 5200 pF, h = 2 mm; 5) C = 5200 pF, h = 0.5 mm; 6) C = 35,000 pF, h = 0.5 mm.

Figure 3 shows the directivity patterns of the generated shear acoustic waves of frequency 5 MHz for various values of the capacitance C and the height h. We see that the angular dependences for shear waves $U_t(\theta)$ have a more complicated shape than in the case of longitudinal waves. The positions of the maxima depend on the discharge technique: The maxima for discharge on the sample are observed at angles $\theta \sim 40°$ for all values of C, and the maxima for discharge on the auxiliary electrode are shifted toward larger angles θ. According to symmetry considerations, when the air shock is incident on the surface of the sample, shear waves should not be excited in the direction of the normal to the surface ($\theta = 0$). In the experiment, however, nonzero minima were observed at $\theta = 0$, evidently because of the influence of deviations of the actual experimental geometry from the ideal symmetrical case.

Measurements of the directivity patterns of Rayleigh waves generated in a spark discharge showe that the patterns are isotropic within the measurement error limits for all the experimental values of C and h, both for discharge on the sample and for discharge on the auxiliary electrode. We have therefore omitted them here.

The directivity patterns of elastic waves generated by a spark discharge can be calculated quantitatively, in principle, by solving the problem of the refraction of a strong divergent shock wave at the interface between a gas and a linearly elastic solid. Since this problem lacks a rigorous solution, we restrict the ensuing discussion to a qualitative interpretation of the plotted experimental curves of $U_{\ell,t}(\theta)$.

For this purpose, we associate the effect of the shock wave on the surface of the solid with a certain effective normal force F_n, which depends on the distance ρ from the epicenter and on the time, whereupon the generation of elastic waves in a solid half-space can be reduced to the axisymmetrical Lamb problem[10,11] for the effective force $F_n(t, \rho)$. The dependence of this force on the coordinates and on the time must clearly exhibit a lagged (wave) behavior $F_n(t, \rho) = F_n[t - \rho/v(\rho)]$, being determined by the path traced by the shock wave on the plane. Introducing the height ℓ of the lower boundary of the discharge zone above the plane and the distance $r = (\rho^2 + \ell^2)^{1/2}$ from the lower boundary of the discharge zone to the observation point, we see at once that the velocity $v(\rho)$ of the pulse representing the effective normal force along the surface is related to the velocity $v(r)$ of the spherical shock front by the equation $v(\rho) = d\rho/dt = v(r)(1 + h^2/\rho^2)^{1/2}$. In turn, $v(r) \sim (E/\rho_0)^{1/2} r^{-3/2}$, where E is the electrical discharge energy spent in generation of the shock wave, and ρ_0 is the equilibrium air density.[12,13] The pressure $p(r)$ at the shock front is known to be related to $v(r)$ by the equation $p(r) \sim \rho_0 v^2(r) \sim r^{-3} = (\rho^2 + \ell^2)^{-3/2}$. Consequently, the force $F_n(t, \rho)$, which is of the same order of magnitude as $p(r)$, must clearly decrease rapidly as ρ is increased.

In the case of discharge on the samle it can be assumed that $\ell = 0$, and so $r = \rho$. The velocity $v(\rho)$ now decreases as $\rho^{-3/2}$ to the value of the sound velocity in air c_0 (Refs. 7 and 12). Accordingly, the pressure $p(\rho)$ is proportional to ρ^{-3} initially and then varies $\sim\rho^{-1}$. In the case of discharge on the auxiliary electrode $\ell = h$, and

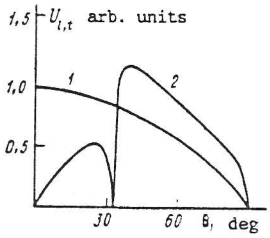

FIG. 4. Calculated directivity patterns of longitudinal (curve 1) and shear (curve 2) waves generated by a vertical lumped force in an elastic half-space.

the function $v(\rho) \sim (\rho^2 + h^2)^{-3/4} (1 + h^2/\rho^2)^{1/2} = \rho^{-3/4} (1 + h^2/\rho^2)^{-1/4}$ decreases somewhat more slowly at small values of ρ. More significant, however, is the fact that the pressure $p(\rho) \sim (\rho^2 + h^2)^{-3/2}$ in this case does not have a singularity in the limit $\rho \to 0$, but is characterized by a plateau of radius $\rho_p \sim h$ in the neighborhood of the epicenter. In other words, the distributed character of the force source $F_n(t, \rho)$ in the case of discharge on the auxiliary electrode is manifested more explicitly than in the case of discharge on the sample, where the source can clearly be regarded as a point source.

For comparison, Fig. 4 shows the calculated directivity patterns of longitudinal (curve 1) and shear (curve 2) waves generated by a vertical lumped force (point source) in an elastic half-space[11] for a Poisson ratio $\sigma = 0.35$, which corresponds to aluminum. We first compare the theoretical curve for shear waves with the corresponding experimental curves of $U_t(\theta)$ in the case of discharge directly on the sample (Fig. 3, curve 1-3). We see that curve 2 in Fig. 4 and curves 1-3 in Fig. 3 are qualitatively similar, consistent with the assumption that the source is a point source.

In the case of discharge on the auxiliary electrode, on the other hand, the observed changes in the behavior of the experimental curves (curves 4-6 in Fig. 3) are obviously associated with the lagged character of the force $F_n = F_n[t - \rho/v(\rho)]$, which can exert an appreciable influence in the case of a distributed source. Indeed, according to previous experimental data,[7] the velocity of the shock wave $v|_{r=h} = 1000$ m/s at a height h equal (e.g.) to 0.2 mm. In accordance with the foregoing discussion, the velocity of its trace on the surface $v(\rho) = v|_{r=h}(1 + h^2/\rho^2)^{1/2}$ can be considerably higher than 1000 m/s near the epicenter (at $\rho \lesssim h$). In particular, the velocity $v(\rho)$ can also exceed the shear bulk wave velocity c_t in the solid ($c_t \approx 3100$ m/s for aluminum), which evidently accounts for the onset of the additional maxima of curves 5 and 6 in Fig. 3 at $\theta \sim 70°$. The form of the $U_t(\theta)$ curve (curve 4) also differs from the theoretical curve in Fig. 4 for an electrode height h = 2 mm, but the pronounced maximum at large θ is not observed here. Its absence can probably be attributed to the fact that the velocity of the shock wave is close to the sound velocity in air $c_0 \approx 340$ m/s as it approaches the surface in this case, and the velocity $v(\rho)$ exceeds the velocity c_t only in a small neighborhood of the epicenter.

We now discuss the directivity characteristic $U_\ell(\theta)$ for longitudinal waves (Fig. 2). In this case all the experimental curves decrease monotonically as the angle θ decreases, both in the case of discharge on the sample (curves 1-4) and in the case of discharge on the auxiliary electrode (curves 5-7); this result agrees with the theoretical curve in Fig. 4, which is calculated for a lumped force. In regard to the experimental curves 1-4, this fact confirms the point character of the source in discharge on the sample. On the other hand, the absence of any appreciable singularities of curves 5-7 can be attributed to the larger value of the longitudinal wave velocity c_ℓ in comparison with the shear wave velocity (c_ℓ = 6400 m/s for aluminum), so that it is difficult for the effective force $F_n(t, \rho)$ to exhibit a lagged behavior.

We note that the point nature of the spark source in the case of discharge on the sample has also been concluded by Copper et al.[6] on the basis of a measurement of the angular dependence for the generated longitudinal waves. However, our analysis shows that measurements limited to longitudinal waves are not sufficient for arriving at this (as it happens) correct conclusion with certainty, because even in the case of a distributed source (for discharge on the auxiliary electrode) the directivity pattern for longitudinal waves (curves 5-7) have a similar form. The additional shear wave measurements reported in the present study permit the conclusion of the point character of the spark source in the case of discharge on the sample to be drawn with absolute certainty.

Thus, the experimental directivity patterns obtained here for a spark source of acoustic waves in a solid contain important information about the distinctive features of the processes of spark sound generation for two principal discharge geometries. Of course, the measured directivity patterns can also be used directly in practice in connection with the application of spark sources in ultrasonic diagnostic problems.

[1] D. Hutchins, J. Hu, and K. Lundgren, Mater. Eval. 44, 1244 (1986).
[2] A. N. Vasil'ev, Vestn. Mosk. Univ. Fiz. Astron. 28, 54 (1987).
[3] A. A. Karabutov, Usp. Fiz. Nauk 147, 605 (1985) [Sov. Phys. Usp. 28, 1042 (1985)].
[4] V. V. Krylov, E. P. Ponomarev, and T. V. Shtentsel', Vestn. Mosk. Univ. Fiz. Astron. 27, 43 (1986).
[5] A. I. Kozlov and V. P. Plesskii, Fiz. Tverd. Tela (Leningrad) 28, 9 (1986) [Sov. Phys. Solid State 28, 4 (1986)].
[6] J. A. Cooper, R. J. Dewhurst, P. S. Moody, and S. B. Palmer, Proc. Inst. Electr. Eng. 131, 275 (1984).
[7] S. V. Korolev, V. A. Krasil'nikov, and V. V. Krylov, Akust. Zh. 33, 774 (1987) [Sov. Phys. Acoust. 33, 451 (1987)].
[8] S. V. Korolev and V. V. Krylov, "Generation of elastic waves by spark breakdown of a surface gas layer," in: Third Scientific and Technical Conference on the Application of Modern Methods in Nondestructive Testing and Inspection [in Russian], Dal'standart, Khabarovsk (1987), pp. 190-191.
[9] S. V. Korolev and V. V. Krylov, "Spark discharge near a surface: a new and effective method for the noncontact generation of Rayleigh waves," in: Proceedings of the Conference on Acoustoelectronic Information-Processing Devices (Cherkassy, 1988) [in Russian], VINITI, Moscow (1988), pp. 287-288.
[10] W. Nowacki, Theory of Elasticity [Russian translation], Mir, Moscow (1975); Teoria Pelzania, Arkady, Warsaw (1963).
[11] J. E. White, Seismic Waves: Radiation, Transmission, and Attenuation, McGraw-Hill, New York (1965).
[12] Ya. B. Zel'dovich, and Yu. P. Raizer, Physics of Shock Waves and High Temperature Hydrodynamic Phenomena, 2 Vols., Academic Press, New York (1966, 1967).
[13] K. A. Naugol'nykh and N. A. Roi, Electrical Discharges in Water [in Russian], Nauka, Moscow (1971).

Translated by J. S. Wood